Published in final edited form as:
Science. 2014 February 14; 343(6172): 783–787. doi:10.1126/science.1248465.

A viral RNA structural element alters host recognition of non-self RNA

Jennifer L. Hyde[1], **Christina L. Gardner**[2], **Taishi Kimura**[3], **James P. White**[1], **Gai Liu**[5], **Derek W. Trobaugh**[2], **Cheng Huang**[4], **Marco Tonelli**[6], **Slobodan Paessler**[4], **Kiyoshi Takeda**[3], **William B. Klimstra**[2], **Gaya K. Amarasinghe**[5], and **Michael S. Diamond**[1,5,7]

[1]Department of Medicine Washington University School of Medicine, St Louis. MO 63110 USA.

[2]Department of Microbiology and Molecular Genetics, Center for Vaccine Research, University of Pittsburgh, Pittsburgh, PA 15261 USA.

[3]Laboratory of Immune Regulation, Graduate School of Medicine, Osaka University, 2-2 Yamadaoka, Suita, Osaka 565-0871, Japan.

[4]Department of Pathology, University of Texas Medical Branch at Galveston, Galveston, TX 77555 USA.

[5]Department of Pathology & Immunology, Washington University School of Medicine, St Louis. MO 63110 USA.

[6]National Magnetic Resonance Facility at Madison, University of Wisconsin, Madison, 433 Babcock Drive, Madison, WI 53706 USA.

[7]Department of Molecular Microbiology, Washington University School of Medicine, St Louis. MO 63110 USA.

Abstract

Although interferon (IFN) signaling induces genes that limit viral infection, many pathogenic viruses overcome this host response. As an example, *2′-O* methylation of the 5′ cap of viral RNA subverts mammalian antiviral responses by evading restriction of Ifit1, an IFN-stimulated gene that regulates protein synthesis. However, alphaviruses replicate efficiently in cells expressing Ifit1 even though their genomic RNA has a 5′ cap lacking *2′-O* methylation. We show that pathogenic alphaviruses use secondary structural motifs within the 5′-untranslated region (UTR) of their RNA to alter Ifit1 binding and function. Mutations within the 5′-UTR affecting RNA structural elements enabled restriction by or antagonism of Ifit1 *in vitro* and *in vivo*. These results identify an evasion mechanism by which viruses use RNA structural motifs to avoid immune restriction.

Eukaryotic mRNA contains a 5′ cap structure with a methyl group at the *N-7* position (cap 0). In higher eukaryotes, methylation also occurs at the *2′-O* position of the penultimate and antepenultimate nucleotides to generate cap 1 and 2 structures, respectively. Many viral

Corresponding author: Michael S. Diamond, M.D., PhD, Departments of Medicine, Molecular Microbiology and Pathology & Immunology, Washington University School of Medicine, 660 South Euclid Avenue, Box 8051, St Louis. Missouri 63110. Tel: 314-362-2842, Fax: 314-362-9230, diamond@borcim.wustl.edu.

mRNA also display cap 1 structures. Because cytoplasmic viruses cannot use host nuclear capping machinery, some have evolved viral methyltransferases for *N-7* and *2′-O* capping or mechanisms to "steal" the cap from host mRNA (*1*). Whereas *N-7* methylation of mRNA is critical for efficient translation (*2*), cytoplasmic viruses encoding mutations in their viral *2′-O*-methyltransferases are inhibited by IFIT proteins (*3-7*), a family of IFN-stimulated genes (ISGs) induced after viral infection (reviewed in (*8*)). Thus, *2′-O* methylation of host mRNA likely evolved in part, to distinguish self from non-self RNA (*9, 10*).

Alphaviruses are positive strand RNA viruses that replicate in the cytoplasm, lack *2′-O* methylation on the 5′ end of their genomic RNA (*11, 12*), and thus should be restricted by IFIT proteins. To assess the role of IFIT1 in limiting alphavirus replication we silenced its expression in human HeLa cells and then infected with Venezuelan equine encephalitis virus (VEEV) strain TC83, an attenuated New World alphavirus. In cells with reduced IFIT1 expression, TC83 replicated to higher levels (Fig 1A). To determine whether this phenotype occurred *in vivo*, wild-type (WT) and *Ifit1*$^{-/-}$ C57BL/6 mice were infected with TC83. In contrast to WT mice, *Ifit1*$^{-/-}$ mice succumbed to TC83 infection (Fig 1B) and sustained higher viral burden (Fig 1C and D; Fig S1), especially in the brain and spinal cord.

We next analyzed the growth of TC83 in mouse embryonic fibroblasts (MEFs). Although untreated WT and *Ifit1*$^{-/-}$ MEFs supported TC83 infection equivalently (Fig 1E), IFNβ pre-treatment preferentially inhibited replication in WT cells. However, an absence of Ifit1 was sufficient to restore infection. A similar trend was observed with *Ifit1*$^{-/-}$ dendritic cells and cortical neurons (Fig S2A and B). TC83 infection in *Ifit1*$^{-/-}$ MEFs remained partially inhibited by IFNβ treatment, indicating that additional ISGs restrict viral replication (*13-15*). The similarity of infection by TC83 in untreated WT and *Ifit1*$^{-/-}$ MEFs likely reflects the ability of alphaviruses to antagonize induction of type I IFN and ISGs (*16, 17*).

TC83 was generated after passage of the virulent Trinidad donkey (TRD) VEEV strain and contains two changes that attenuate virulence (*18*). One mutation occurs at nucleotide 3 (nt 3, G3A) in the 5′-UTR and increases the sensitivity of TC83 to type I IFN (*17*). We hypothesized that that 5′-UTR mutation might explain the differential sensitivity to Ifit1 and pathogenicity of TC83 and TRD. To begin to test this hypothesis, WT and *Ifit1*$^{-/-}$ mice were infected with TRD (Fig 1F). WT and *Ifit1*$^{-/-}$ mice succumbed to TRD infection without differences in survival time or mortality. Thus, in contrast to TC83, TRD was relatively resistant to the antiviral effects of Ifit1.

To determine if the effect of the G3A mutation was independent of the TC83 structural genes, which contain a second attenuating mutation (*19*), we assessed replication in WT and *Ifit1*$^{-/-}$ MEFs of two isogenic chimeric VEEV/Sindbis (SINV) viruses (*20*); these encode the 5′-UTR and non-structural proteins of TRD and structural proteins of SINV, and differ only at nt 3 ((G3)VEE/SINV and (A3)VEE/SINV) (Fig S3A and B). In IFNβ pre-treated WT MEFs, (A3)VEE/SINV was not recovered from culture supernatants (Fig 2A). However, in IFNβ-treated *Ifit1*$^{-/-}$ MEFs, (A3)VEE/SINV infection was partially restored. In contrast, (G3)VEE/SINV replicated equivalently in IFNβ treated WT and *Ifit1*$^{-/-}$ MEFs (Fig 2B), indicating that a G at nt 3 renders VEEV resistant to inhibition by Ifit1.

RNA secondary structure algorithms predicted differences in base pairing at the 5′ end of the UTR of G3 and A3 RNA (Fig S3A and (*20, 21*)). The imino region of a 2D NOESY NMR spectrum revealed that A3 RNA displayed less secondary structure and base pairing than G3 RNA (Fig S4A and B) and fewer cross peaks in the corresponding 1H/15N Heteronuclear Single Quantum Coherence (HSQC) spectrum (Fig S4C and D). On the basis of these data, we hypothesized that the stable stem-loop structure in the 5′-UTR of TRD compensated for the absence of *2′-O* methylation of alphavirus RNA. To determine whether the secondary structure or primary sequence modulated Ifit1 susceptibility, we analyzed the growth of VEE/SINV containing the A3 nt mutation that also had compensatory mutations that were predicted to restore the 5′-UTR stem-loop (Fig 2C and D; Fig S3C). Although two of the mutants tested (A3U24 and A3U24;A20U) showed increased (relative to (A3)VEE/SINV) but limited growth in IFNβ-treated WT MEFs, a third mutant (A3U24;20_21insC) infected to levels comparable to (G3)VEE/SINV in IFNβ-treated WT and *Ifit1*$^{-/-}$ MEFs. Mutants that replicated less well in IFNβ-treated WT MEFs (A3U24 and A3U24;A20U) were predicted to have less stable minimum free energy structures relative to (A3U24;20_21insC)VEE/SINV and (G3)VEE/SINV. To further define the requirements in the 5′-UTR for evasion of Ifit1 restriction, we evaluated additional viral mutants: one that changed the sequence of the A3U24 loop but retained the less stable stem structure of the parent A3U24 5′-UTR ((LOOP)VEE/SINV) (*21*), and two G3 variants with more stable hairpins (G3;C19C20)VEE/SINV that contained additional nucleotide repeats (AUG and AUG_2) appended to the 5′-end (Fig S5A). The latter (AUG_n)VEE/SINV mutants were relevant as RNA recognition by IFIT proteins reportedly requires a 5′-overhang of three to five nucleotides (*22*). Alteration of the loop sequence ((LOOP)VEE/SINV) did not relieve Ifit1-mediated restriction (Fig S5B). However, G3 mutants with an overhang of three or more nucleotides at the 5′-end became sensitive to Ifit1-dependent antiviral effects (Fig S5C).

To assess whether nucleotide changes altered the stability of the VEEV 5′-UTR, we monitored RNA unfolding by circular dichroism spectrometry (Fig S6). Changes in ellipticity as a function of temperature were analyzed (Fig 2E-I and Table S1); we observed several maxima, presumably corresponding to major cooperative unfolding events (Fig 2E-I). We detected more pronounced maxima near 75°C in all but the A3 RNA, confirming that A3 and G3 RNA have different stabilities. The A3U24;20_21insC mutant RNA displayed the most stable secondary structure. Computational analyses suggested that even closely related RNA sequences (i.e., A3 and A3U24) have different ensemble free energy and diversity (see Table S2). Differences in the base pairing probability were noted, which further support structural differences between A3 and G3 RNA (Fig S7). We also measured T_m values (Table S1), which showed an inverse correlation between Ifit1 susceptibility and base-pairing stability. These analyses suggest that G3 and A3U24;20_21insC 5′-UTR RNA adopt more stable conformations, which correlates with antagonism of Ifit1.

To validate that changes at nt 3 determined sensitivity to Ifit1 independently of other VEEV-encoded factors, we repeated experiments with isogenic variants of TC83 and an enzootic VEEV strain, ZPC-738 (Fig 3A-D; Fig S3D). Whereas TC83 replicated poorly in IFNβ treated WT MEFs, the isogenic nt 3 mutant TC83 A3G showed increased replication (Fig 3A), confirming that the A3G mutation confers resistance to type I IFN. However, unlike

that seen with (G3)VEE/SINV (Fig 2B), the phenotype of TC83 A3G in IFNβ-treated WT MEFs did not fully recapitulate the restoration seen in IFNβ-treated *Ifit1*$^{-/-}$ MEFs (compare Fig 3A to 3B), suggesting that additional viral elements may be inhibited by Ifit1. Infection of the mutant ZPC-738 G3A in IFNβ-treated WT MEFs was decreased compared to WT ZPC-738 whereas infection of WT and G3A ZPC-738 was equivalent in IFNβ treated *Ifit1*$^{-/-}$ MEFs (Fig 3C and D).

To assess whether nt 3 mutation reciprocally affects virulence, we infected WT and *Ifit1*$^{-/-}$ mice with, TC83, ZPC-738, and paired isogenic variants (Fig 3E and F). In WT mice, ZPC-738 G3A was attenuated compared to the WT virus. However, no difference in mortality and only a small difference in survival kinetics were observed in *Ifit1*$^{-/-}$ mice infected with ZPC-738 WT or G3A. In comparison, we observed increased lethality in WT mice infected with TC83 A3G relative to TC83. We also noted a slight decrease in survival kinetics of *Ifit1*$^{-/-}$ mice infected with A3G as compared to TC83 WT, suggesting that the A3G change may have additional effects aside from antagonizing Ifit1 function.

To determine whether structures in the 5′-UTR of other alphaviruses functioned analogously, we introduced mutations at either nt 5 or 8 into SINV (Fig 3G and H; Fig S3E). These mutations were selected because they altered the virulence of SINV in rats (*23, 24*) and were predicted to change the 5′-UTR secondary structure (Fig S3E). An A to G substitution at nt 5 resulted in increased viral replication relative to parental virus in IFNβ-pre-treated WT MEFs but not in IFNβ-treated *Ifit1*$^{-/-}$ MEFs, suggesting that the A5G phenotype was specific to Ifit1. Conversely, a substitution at nt 8 (G8U) resulted in a decrease in replication in IFNβ-treated WT MEFs relative to WT SINV, which was restored to comparable levels in IFNβ-treated *Ifit1*$^{-/-}$ MEFs. This experiment establishes that mutations within the 5′-UTR of an Old World alphavirus also affect Ifit1 antagonism, suggesting that secondary structure at the 5′-UTR might be a more universal mechanism to circumvent Ifit1-mediated restriction.

IFIT1 binds flavivirus RNA lacking *2′-O* methylation and blocks translation and binding of eukaryotic translation initiation factors (*6, 7, 25*). To determine whether Ifit1 differentially affected translation of alphavirus RNA with different 5′-UTR RNA structures, we transfected type 0 capped WT and G3A mutant translation reporter RNA encoding a luciferase gene fused to nsP1 (Fig S3F) (*26*) into IFNβ-treated or untreated MEFs (Fig 4A-D). In WT MEFs treated with IFNβ (Fig 4A), G3 RNA exhibited greater translation reporter activity relative to A3 RNA. We also detected greater translation of G3 reporter RNA in untreated WT MEFs (Fig 4B), suggesting that basal Ifit1 expression in these cells may limit A3 RNA translation. However, we observed a greater increase in A3 reporter RNA translation relative to G3 in *Ifit1*$^{-/-}$ MEFs that were treated with IFNβ or left untreated (Fig 4C and D). The higher level of A3 versus G3 RNA translation in *Ifit1*$^{-/-}$ MEFs was not unexpected, as (A3)VEE/SINV replicates more efficiently than (G3)VEE/SINV in cells lacking type I IFN induction (*20*). Although A3 RNA has a translation advantage in cells defective for innate immune responses, the G3 residue confers resistance to Ifit1.

We hypothesized that alphavirus mutants with different 5′-UTR structural stabilities might interact with Ifit1 in a manner that is less compatible with translation. We used

electrophoretic mobility shift assays (EMSA) (Fig 4E-G) to determine whether TRD 5′-UTR RNA containing an A3 or G3 and a type 0 cap differentially interacted with Ifit1 (Fig 4E). We observed significant binding of Ifit1 to A3 RNA, but less binding to G3 RNA suggesting that the secondary structure of the G3 RNA likely inhibited interaction with Ifit1. This conclusion was supported by dot-blot binding studies, which showed a 2 to 10-fold greater affinity (K_D ~ 30 nM) of cap 0 A3 RNA compared to G3 RNA for Ifit1, depending on the incubation conditions (Fig 4H and Fig S8). The binding of Ifit1 to cap 0 RNA was specific, as it was competed by excess unlabeled 5′-ppp A3 RNA (Fig S7). Exogenous *2′-O* methylation of A3 and G3 RNA, which generates a type 1 cap, resulted in less Ifit1 binding (Fig 4F), which agrees with flavivirus studies (*6, 7*). When EMSA experiments were repeated in the absence of capping, TRD 5′-UTR RNA containing an A3 or G3 and a free 5′-ppp differentially and weakly recognized Ifit1 (Fig 4G), consistent with experiments demonstrating that ssRNA, but not dsRNA containing a free 5′-ppp is bound by IFIT1 (*22*). Excess A3 5′-ppp RNA compared to G3 5′-ppp RNA preferentially competed for Ifit1 binding to type 0 cap A3 RNA (K_i of 3 μM and 48 μM for A3 and G3 5′-ppp RNA, respectively; Fig S9). These results suggest that secondary structure in the context of an uncapped RNA can alter Ifit1 binding and may contribute to why negative-stranded viruses with 5′-ppp genomic RNA and highly structured 5′-UTRs (e.g., filoviruses) are resistant to type I IFN and Ifit1-mediated control. Our results also establish that Ifit1 has a higher affinity for RNA with a type 0 cap compared to a free 5′-ppp moiety.

In summary, alphaviruses use a stable 5′-UTR stem-loop structure to antagonize Ifit1 antiviral activity. Although some IFIT proteins bind 5′-ppp RNA (*22, 27*), it remains to be determined how Ifit1 differentially recognizes capped RNA that display or lack 2′-O methylation, and how alphavirus 5′-UTR stem-loop structures impacts this. Our experiments suggest that genomic RNA elements can function to evade host cell-intrinsic immunity. Thus, structural elements in viral or virus-associated RNA can bind antiviral proteins irreversibly to block function (*28, 29*) or attenuate binding of host antiviral proteins. It is intriguing to consider that viral RNA structural elements that antagonize Ifit1 recognition may have become targets for other RNA sensors (e.g., RIG-I and MDA5). Finally, these results may be relevant to pharmaceutical approaches that use mRNA as therapeutics or vaccine design strategies for attenuating alphaviruses and other viruses.

Supplementary Material

Refer to Web version on PubMed Central for supplementary material.

Acknowledgments

NIH grants U19 AI083019 (M.S.D.), R01 AI104972 (M.S.D.), R01 AI083383 (W.B.K.) and Training Grant AI049820 (D.W.T.), and the Institute for Human Infections and Immunity, University of Texas Medical Branch (S.P) supported this work. The authors wish to thank I. Frolov, M. MacDonald, and C. Rice for their generosity with alphavirus reagents and experimental advice. This study made use of the National Magnetic Resonance Facility at Madison, which is supported by NIH grants P41RR02301 (BRTP/NCRR) and P41GM66326 (NIGMS). The luciferase reporter gene constructs and virulent VEEV strains are subject to Material Transfer Agreements with the University of Pittsburgh and the University of Texas Medical Branch, respectively. The virulent VEEV strain (TRD) requires BSL3 facilities and USDA approval. The authors have no financial conflicts to disclose. The data reported in this manuscript are tabulated in the main paper and in the supplementary materials.

REFERENCES

1. Plotch SJ, Bouloy M, Ulmanen I, Krug RM. A unique cap(m7GpppXm)-dependent influenza virion endonuclease cleaves capped RNAs to generate the primers that initiate viral RNA transcription. Cell. Mar.1981 23:847. [PubMed: 6261960]
2. Muthukrishnan S, Both GW, Furuichi Y, Shatkin AJ. 5′-Terminal 7-methylguanosine in eukaryotic mRNA is required for translation. Nature. May 1.1975 255:33. [PubMed: 165427]
3. Daffis S, et al. 2′-O methylation of the viral mRNA cap evades host restriction by IFIT family members. Nature. 2010; 468:452. [PubMed: 21085181]
4. Zust R, et al. Ribose 2′-O-methylation provides a molecular signature for the distinction of self and non-self mRNA dependent on the RNA sensor Mda5. Nat Immunol. Feb.2011 12:137. [PubMed: 21217758]
5. Szretter KJ, et al. 2′-O methylation of the viral mRNA cap by West Nile virus evades Ifit1-dependent and -independent mechanisms of host restriction in vivo. PLoS Pathog. 2012; 8:e1002698. [PubMed: 22589727]
6. Kimura T, et al. Ifit1 inhibits JEV replication through binding to 5′ capped 2′-O unmethylated RNA. J Virol. Jul 3.2013 87:9997. [PubMed: 23824812]
7. Habjan M, et al. Sequestration by IFIT1 Impairs Translation of 2′O-unmethylated Capped RNA. PLoS Pathog. Oct.2013 9:e1003663. [PubMed: 24098121]
8. Diamond MS, Farzan M. The broad-spectrum antiviral functions of IFIT and IFITM proteins. Nat Rev Immunol. Jan.2013 13:46. [PubMed: 23237964]
9. Wei CM, Gershowitz A, Moss B. Methylated nucleotides block 5′ terminus of HeLa cell messenger RNA. Cell. Apr.1975 4:379. [PubMed: 164293]
10. Wei CM, Moss B. Methylated nucleotides block 5′-terminus of vaccinia virus messenger RNA. Proc Natl Acad Sci U S A. Jan.1975 72:318. [PubMed: 164018]
11. Hefti E, Bishop DH, Dubin DT, Stollar V. 5′ nucleotide sequence of sindbis viral RNA. J Virol. Jan.1975 17:149. [PubMed: 173879]
12. Pettersson RF, Soderlund H, Kaariainen L. The nucleotide sequences of the 5′-terminal T1 oligonucleotides of Semliki-Forest-virus 42-S and 26-S RNAs are different. Eur J Biochem. Apr. 1980 105:435. [PubMed: 7371641]
13. Schoggins JW, et al. A diverse range of gene products are effectors of the type I interferon antiviral response. Nature. 2011; 472:481. [PubMed: 21478870]
14. Karki S, et al. Multiple interferon stimulated genes synergize with the zinc finger antiviral protein to mediate anti-alphavirus activity. PloS one. 2012; 7:e37398. [PubMed: 22615998]
15. Zhang Y, Burke CW, Ryman KD, Klimstra WB. Identification and characterization of interferon-induced proteins that inhibit alphavirus replication. J Virol. Oct.2007 81:11246. [PubMed: 17686841]
16. Yin J, Gardner CL, Burke CW, Ryman KD, Klimstra WB. Similarities and differences in antagonism of neuron alpha/beta interferon responses by Venezuelan equine encephalitis and Sindbis alphaviruses. J Virol. Oct.2009 83:10036. [PubMed: 19641001]
17. White LJ, Wang JG, Davis NL, Johnston RE. Role of alpha/beta interferon in Venezuelan equine encephalitis virus pathogenesis: effect of an attenuating mutation in the 5′ untranslated region. J Virol. Apr.2001 75:3706. [PubMed: 11264360]
18. Kinney RM, et al. Attenuation of Venezuelan equine encephalitis virus strain TC-83 is encoded by the 5′-noncoding region and the E2 envelope glycoprotein. J Virol. 1993; 67:1269. [PubMed: 7679745]
19. Johnson BJ, Kinney RM, Kost CL, Trent DW. Molecular determinants of alphavirus neurovirulence: nucleotide and deduced protein sequence changes during attenuation of Venezuelan equine encephalitis virus. J Gen Virol. Sep.1986 67(Pt 9):1951. [PubMed: 3755750]
20. Kulasegaran-Shylini R, Thiviyanathan V, Gorenstein DG, Frolov I. The 5′UTR-specific mutation in VEEV TC-83 genome has a strong effect on RNA replication and subgenomic RNA synthesis, but not on translation of the encoded proteins. Virology. Apr 25.2009 387:211. [PubMed: 19278709]

21. Kulasegaran-Shylini R, Atasheva S, Gorenstein DG, Frolov I. Structural and functional elements of the promoter encoded by the 5′ untranslated region of the Venezuelan equine encephalitis virus genome. J Virol. Sep.2009 83:8327. [PubMed: 19515761]
22. Abbas YM, Pichlmair A, Gorna MW, Superti-Furga G, Nagar B. Structural basis for viral 5′-PPP-RNA recognition by human IFIT proteins. Nature. Feb 7.2013 494:60. [PubMed: 23334420]
23. Kobiler D, et al. A single nucleotide change in the 5′ noncoding region of Sindbis virus confers neurovirulence in rats. J Virol. Dec.1999 73:10440. [PubMed: 10559362]
24. McKnight KL, et al. Deduced consensus sequence of Sindbis virus strain AR339: mutations contained in laboratory strains which affect cell culture and in vivo phenotypes. J Virol. Mar.1996 70:1981. [PubMed: 8627724]
25. Kumar P, et al. Inhibition of translation by IFIT family members is determined by their ability to interact selectively with the 5′-terminal regions of cap0-, cap1- and 5′ppp-mRNAs. Nucleic Acids Res. Dec 25.2013
26. Tesfay MZ, et al. Alpha/beta interferon inhibits cap-dependent translation of viral but not cellular mRNA by a PKR-independent mechanism. J Virol. Mar.2008 82:2620. [PubMed: 18160435]
27. Pichlmair A, et al. IFIT1 is an antiviral protein that recognizes 5′-triphosphate RNA. Nat Immunol. Jul.2011 12:624. [PubMed: 21642987]
28. O'Malley RP, Mariano TM, Siekierka J, Mathews MB. A mechanism for the control of protein synthesis by adenovirus VA RNAI. Cell. Feb 14.1986 44:391. [PubMed: 3943131]
29. Kitajewski J, et al. Adenovirus VAI RNA antagonizes the antiviral action of interferon by preventing activation of the interferon-induced eIF-2 alpha kinase. Cell. Apr 25.1986 45:195. [PubMed: 3698097]
30. Roehrig JT, Day JW, Kinney RM. Antigenic analysis of the surface glycoproteins of a Venezuelan equine encephalomyelitis virus (TC-83) using monoclonal antibodies. Virology. Apr 30.1982 118:269. [PubMed: 6178209]
31. Petrakova O, et al. Noncytopathic replication of Venezuelan equine encephalitis virus and eastern equine encephalitis virus replicons in Mammalian cells. J Virol. Jun.2005 79:7597. [PubMed: 15919912]
32. Garmashova N, et al. Analysis of Venezuelan equine encephalitis virus capsid protein function in the inhibition of cellular transcription. J Virol. Dec.2007 81:13552. [PubMed: 17913819]
33. Gardner CL, et al. Eastern and Venezuelan equine encephalitis viruses differ in their ability to infect dendritic cells and macrophages: impact of altered cell tropism on pathogenesis. J Virol. Nov.2008 82:10634. [PubMed: 18768986]
34. Rice CM, Levis R, Strauss JH, Huang HV. Production of infectious RNA transcripts from Sindbis virus cDNA clones: mapping of lethal mutations, rescue of a temperature-sensitive marker, and in vitro mutagenesis to generate defined mutants. J Virol. Dec.1987 61:3809. [PubMed: 3479621]
35. Anishchenko M, et al. Generation and characterization of closely related epizootic and enzootic infectious cDNA clones for studying interferon sensitivity and emergence mechanisms of Venezuelan equine encephalitis virus. J Virol. Jan.2004 78:1. [PubMed: 14671082]
36. Fuchs A, Pinto AK, Schwaeble WJ, Diamond MS. The lectin pathway of complement activation contributes to protection from West Nile virus infection. Virology. Mar 30.2011 412:101. [PubMed: 21269656]
37. Gruber AR, Lorenz R, Bernhart SH, Neubock R, Hofacker IL. The Vienna RNA websuite. Nucleic Acids Res. Jul 1.2008 36:W70. [PubMed: 18424795]
38. Mathews DH, Sabina J, Zuker M, Turner DH. Expanded sequence dependence of thermodynamic parameters improves prediction of RNA secondary structure. J Mol Biol. May 21.1999 288:911. [PubMed: 10329189]
39. Ding Y, Chan CY, Lawrence CE. RNA secondary structure prediction by centroids in a Boltzmann weighted ensemble. RNA. Aug.2005 11:1157. [PubMed: 16043502]
40. McCaskill JS. The equilibrium partition function and base pair binding probabilities for RNA secondary structure. Biopolymers. May-Jun;1990 29:1105. [PubMed: 1695107]
41. Darty K, Denise A, Ponty Y. VARNA: Interactive drawing and editing of the RNA secondary structure. Bioinformatics. Aug 1.2009 25:1974. [PubMed: 19398448]

42. Pace CN. Measuring and increasing protein stability. Trends Biotechnol. Apr.1990 8:93. [PubMed: 1367432]

43. Delaglio F, et al. NMRPipe: a multidimensional spectral processing system based on UNIX pipes. J Biomol NMR. Nov.1995 6:277. [PubMed: 8520220]

44. Johnson BA, Blevins RA. NMR View: A computer program for the visualization and analysis of NMR data. J Biomol NMR. Sep.1994 4:603. [PubMed: 22911360]

45. Daffis S, Samuel MA, Keller BC, Gale M Jr. Diamond MS. Cell-specific IRF-3 responses protect against West Nile virus infection by interferon-dependent and independent mechanisms. PLoS Pathog. 2007; 3:e106. [PubMed: 17676997]

46. Samuel MA, Morrey JD, Diamond MS. Caspase-3 dependent cell death of neurons contributes to the pathogenesis of West Nile virus encephalitis. J Virol. 2007; 81:2614. [PubMed: 17192305]

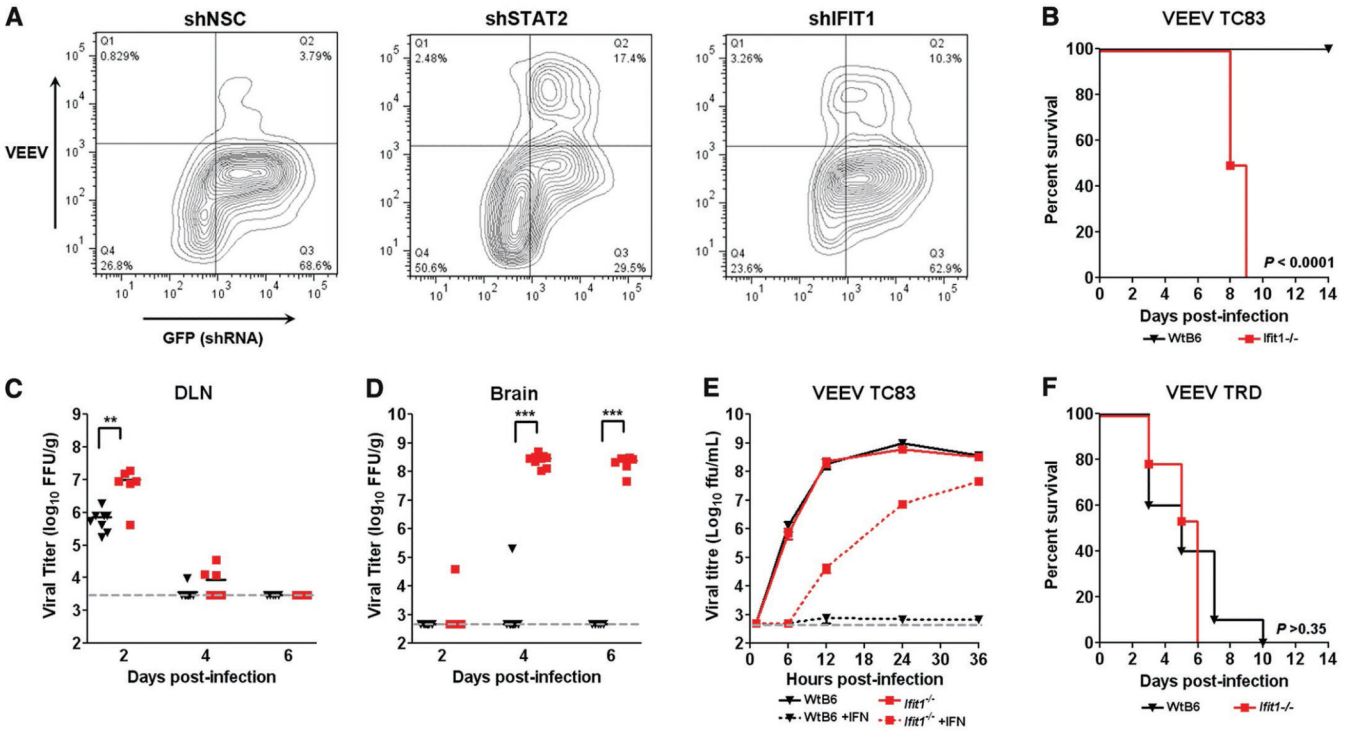

Figure 1. VEEV TC83 but not TRD is restricted by Ifit1

(**A**) Flow cytometry contour plots showing infection of TC83 in IFNβ-treated HeLa cells transduced with shRNA against a scrambled non-silencing control (NSC), human STAT2, or human IFIT1 (shNSC vs. shIFIT1 $P < 0.003$). One representative experiment of four is shown. This phenotype was confirmed with a second shRNA against IFIT1. (**B**) Survival of 4 week-old WT ($n = 10$) and *Ifit1*$^{-/-}$ ($n = 10$) mice after s.c. infection with 10^6 FFU of TC83. Results are pooled from three independent experiments. *P* values for survival were calculated using the Log-rank test. **(C-D)** Viral burden in 4 week-old WT or *Ifit1*$^{-/-}$ mice infected s.c. with 10^6 FFU of TC83, as measured in (**C**) draining popliteal lymph node (DLN) and (**D**) brain. Results are from 5 to 9 mice per tissue. Asterisks indicate statistically significant differences, as judged by an unpaired t test (** $P < 0.005$, *** $P < 0.0001$). Dashed lines indicate the limit of detection of the assay. (**E**) WT and *Ifit1*$^{-/-}$ MEFs were pre-treated with 10 IU/ml of IFNβ for 12 hours or left untreated, and then infected with TC83 (MOI of 0.1). Supernatants were harvested for virus titration (WT versus *Ifit1*$^{-/-}$ $P > 0.2$; WT + IFNβ versus *Ifit1*$^{-/-}$ + IFN, 12, 24, 36 hours post-infection, $P < 0.03$). Each point represents the average of three experiments performed in triplicate, and error bars represent the standard error of the mean (SEM). *P* values were determined by an unpaired t test. (**F**) Survival curves of 8 week-old WT ($n = 10$) and *Ifit1*$^{-/-}$ ($n = 24$) mice after s.c. infection with 50 PFU of TRD. Results are pooled from two independent experiments. *P* values for survival were calculated using the Log-rank test.

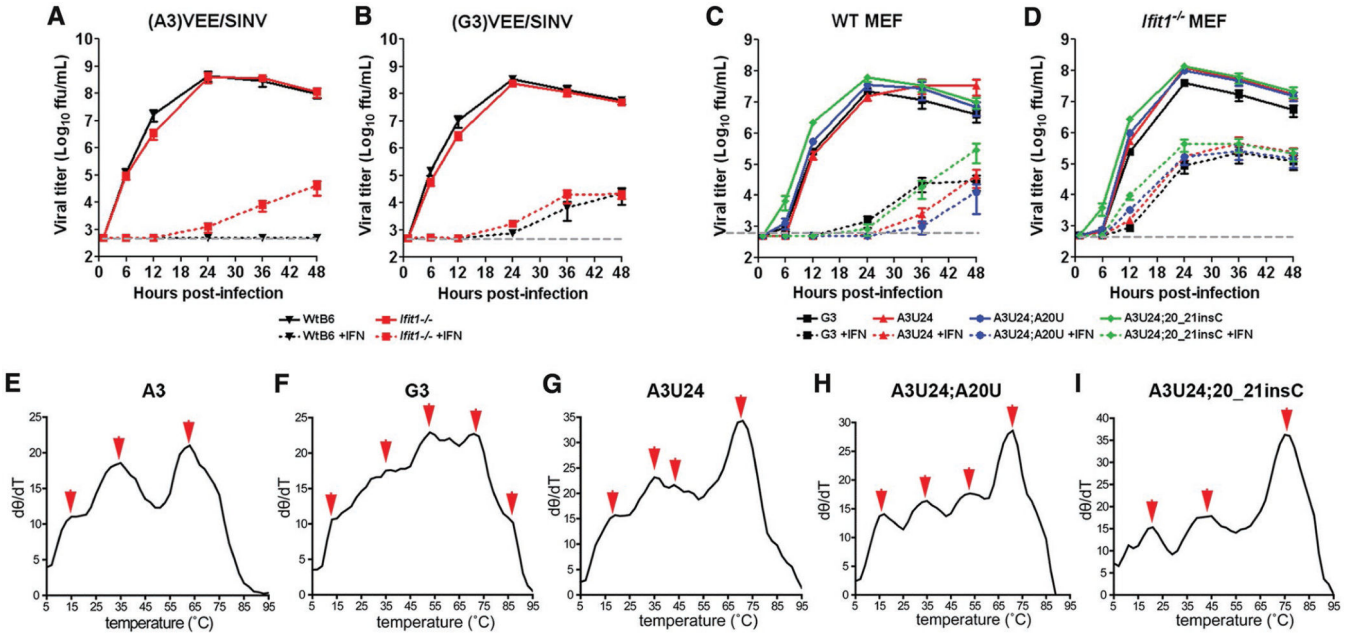

Figure 2. Mutations in the 5′-UTR determine Ifit1 sensitivity *in vitro*. (A and B) Growth kinetics of (A3)VEE/SINV and (G3)VEE/SINV viruses in WT and *Ifit1*$^{-/-}$ MEFs. Cells were pre-treated with 1 IU/ml of IFNβ for 12 hours or left untreated, and then infected with (A3)VEE/SINV or (G3)VEE/SINV (MOI of 0.1). Supernatants were harvested at indicated times for virus titration ((A3)VEE/SINV: WT + IFNβ versus *Ifit1*$^{-/-}$ + IFNβ, 36 and 48 hours post-infection, $P < 0.006$). Each point represents the average of three independent experiments performed in triplicate, and error bars represent SEM. *P* values were determined using an unpaired t-test. Dashed lines indicate the limit of detection of the assay. (**C and D**) Growth kinetics of (G3)VEE/SINV, (A3U24)VEE/SINV, (A3U24;A20U)VEE/SINV, and (A3U24;20_21insC)VEE/SINV viruses in WT (**C**) and *Ifit1*$^{-/-}$ (**D**) MEFs. Experiments and analysis were performed as in panel A. (**E-I**) Thermal denaturation of A3, G3, A3U24, A3U24;A20U, and A3U24;20_21insC RNA as measured by CD at 210 nm. RNA was heated from 5 to 95°C at a rate of 1°C/min and readings were collected every 1°C to monitor unfolding.Data is represented as the change in molar ellipticity as a function of temperature (*dθ/dT*), and red arrows indicate major maxima. One representative experiment of two is shown.

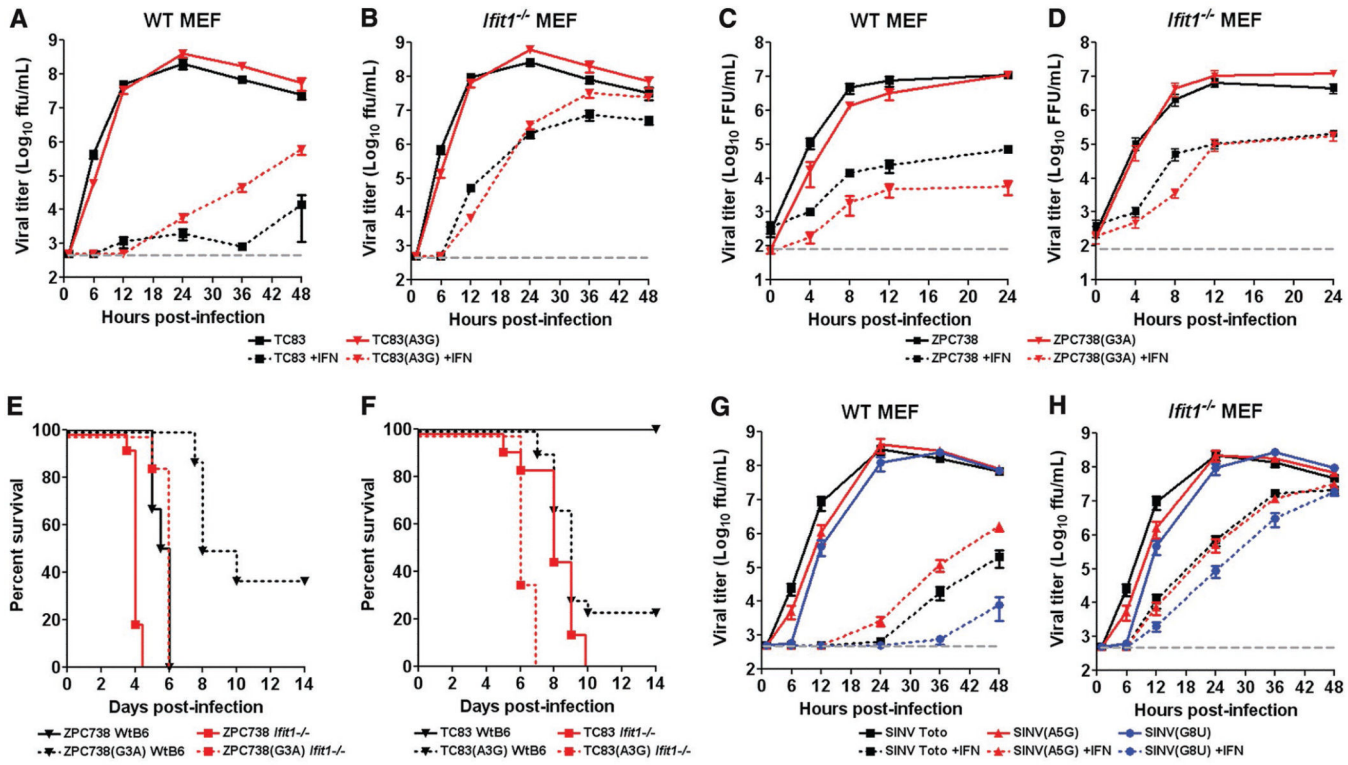

Figure 3. Mutations which alter the secondary structure of the 5′-UTR affect pathogenicity *in vivo*. (A-D)

Growth kinetics of isogenic TC83 WT and A3G (**A and B**) or ZPC-738 WT and G3A (**C and D**) in WT and *Ifit1*$^{-/-}$ MEFs. Cells were pre-treated with 10 IU/ml of IFNβ for 12 hours (TC83) or 100 IU/ml of IFNβ for 8 hours (ZPC738), or left untreated, and then infected with respective viruses (MOI of 0.1). (TC83 versus TC83(A3G): WT + IFNβ, 36 and 48 hours post-infection, $P < 0.006$; ZPC738 vs. ZPC738(G3A): WT + IFNβ, 24 hours post-infection, $P < 0.0001$). Each point represents the average of two (ZPC-738) or three (TC83) independent experiments performed in triplicate, and error bars represent SEM. *P* values were determined using the unpaired t-test. Dashed lines indicate the limit of detection of the assay. (**E and F**) Survival studies of isogenic ZPC-738 WT and G3A (**E**) and TC83 WT and A3G (**F**) viruses in WT and *Ifit1*$^{-/-}$ mice. Mice were infected s.c. with 10^1 PFU of ZPC-738 (WT, $n = 6$; *Ifit1*$^{-/-}$, $n = 15$) or ZPC-738(G3A) (WT, $n = 8$; *Ifit1*$^{-/-}$, $n = 15$) and 10^6 PFU of TC83 (WT, $n = 18$; *Ifit1*$^{-/-}$, $n = 13$) or TC83(A3G) (WT, $n = 21$; *Ifit1*$^{-/-}$, $n = 8$). ZPC738 versus ZPC738(G3A): WT mice, survival $P = 0.0002$; mean time to death (MTD) of 5.5 versus 8.3 days, $P = 0.0002$. ZPC738 versus ZPC738(G3A): *Ifit1*$^{-/-}$ mice, MTD of 4.0 versus 5.8 days, $P < 0.0001$. TC83 versus TC83(A3G): WT mice, survival $P < 0.0001$; TC83 vs. TC83(A3G): *Ifit1*$^{-/-}$ mice, MTD of 8.2 versus 6.3 days, $P < 0.003$. Experiments were performed twice for ZPC-738 viruses and four times for TC83 viruses. *P* values for survival were determined as in Fig 1. *P* values for MTD were determined using an unpaired t-test. (**G and H**) Growth kinetics of SINV Toto, A5G, and G8U SINV in WT (**G**) and *Ifit1*$^{-/-}$ (**H**) MEFs. Cells were pre-treated with 1 IU/ml of IFNβ for 12 hours or left untreated, and then infected with respective viruses at an MOI of 0.1. SINV Toto versus A5G: WT MEFs +

IFNβ, $P < 0.05$; SINV Toto versus G8U, WT MEFs + IFNβ, $P < 0.05$. Experiments and analysis was performed as in panel A.

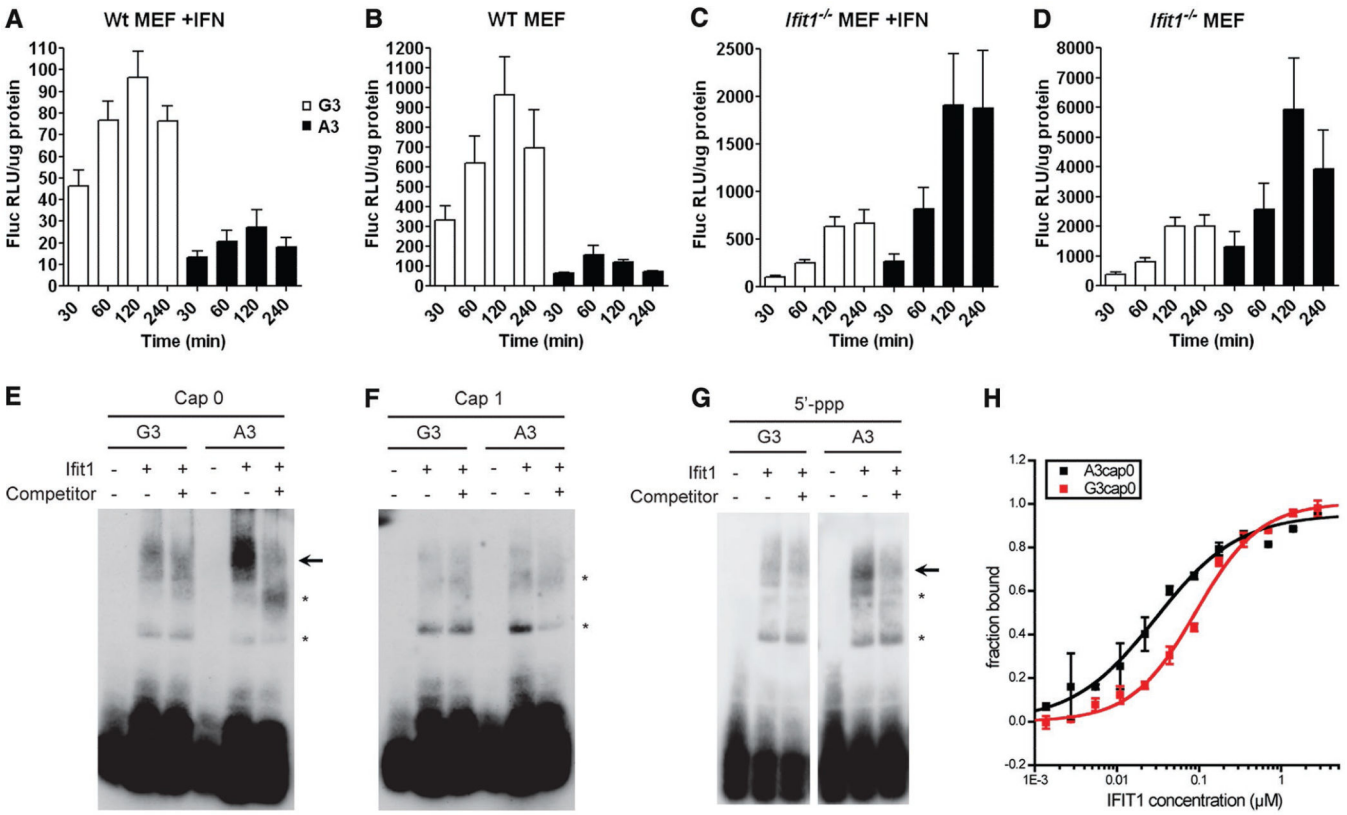

Figure 4. The nt G3 in the 5′-UTR relieves translational inhibition by altering Ifit1-RNA binding. (A-D)

Luciferase assays of A3 and G3 TRD translation reporters. WT and *Ifit1*$^{-/-}$ MEFs were untreated or treated with 100 IU/ml IFNβ for 8 hours, and then electroporated with *in vitro* synthesized and type 0 capped reporter RNA. Cell lysates were harvested at indicated time points and assayed for luciferase activity. Each bar represents the average of four independent experiments performed in triplicate. WT MEFs + IFNβ: G3 versus A3, $P < 0.0004$; WT MEFs, no treatment: G3 versus A3, $P < 0.005$; *Ifit1*$^{-/-}$ MEFs + IFNβ, G3 versus A3, $P < 0.05$ (30, 60, and 120 minutes). Error bars represent the SEM. *P* values were determined using an unpaired t-test. (**E-G**) EMSA of A3 and G3 VEEV 5′-UTR RNA bound to recombinant Ifit1. G3 and A3 VEEV 5′-UTR RNA were synthesized *in vitro* using T7 polymerase (5′-ppp) and then treated with (**E**) an *N-7* methylguanosine capping reagent (Cap 0), (**F**) an *N-7* methylguanosine capping reagent and an exogenous *2′-O* methyltranferase (Cap 1), or (**G**) no enzymes (5′-ppp). All RNA was labeled with biotin and competed with 3 μg of homologous unlabeled RNA. Cap 0 and Cap 1 RNA were heated at 95°C; 5′-ppp RNA were heated at 70°C, as no specific binding was observed after heating at 95°C. Binding assays were performed with 1 μg of Ifit1. EMSA data is representative of at least three independent experiments. Arrows indicate specific binding of RNA to Ifit1 whereas asterisks indicate non-specific binding (not competed with unlabeled RNA). G3 and A3 5′-ppp paired samples were run simultaneously on the same gel and cropped as individual panels for presentation purposes. (**H**) Quantification of Ifit1-A3/G3 RNA binding by filter-binding assay at 4°C. The fraction bound of A3 Cap 0 (black squares) and G3 Cap 0 (red squares) was normalized to maximum binding and plotted against Ifit1 concentration.

Data from A3 (black) and G3 (red) were fitted using the Hill equation. A3 Cap 0 dissociation constant (kD) = 0.030 ± 0.004 μM; G3 Cap 0 kD = 0.091 ± 0.007 μM. One representative experiment of three performed in triplicate is shown.